

Synthesis, Thermal Decomposition Pattern and Single Crystal X-Ray Studies of Dimeric $[\text{Cu}(\text{dmae})(\text{OCOCH}_3)(\text{H}_2\text{O})]_2$: A Precursor for the Aerosol Assisted Chemical Vapour Deposition of Copper Metal Thin Films

Muhammad Mazhar,* S. M. Hussain, Faiz Rabbani, Gabriele Kociok-Köhn,[†] and Kieran C. Molloy[†]

Department of Chemistry, Quaid-i-Azam University, Islamabad-45320, Pakistan. *E-mail: mazhar42pk@yahoo.com

[†]Department of Chemistry, University of Bath, Claverton Down, Bath, BA2 7AY, UK

Received February 21, 2006

A dimeric precursor, $[\text{Cu}(\text{dmae})(\text{OCOCH}_3)(\text{H}_2\text{O})]_2$ for the CVD of copper metal films. (dmaeH = *N,N*-dimethylaminoethanol) was synthesized by the reaction of copper(II) acetate monohydrate ($\text{Cu}(\text{OCOCH}_3)_2 \cdot \text{H}_2\text{O}$) and dmaeH in toluene. The product was characterized by m.p. determination, elemental analysis and X-ray crystallography. Molecular structure of $[\text{Cu}(\text{dmae})(\text{OCOCH}_3)(\text{H}_2\text{O})]_2$ shows that a dimeric unit $[\text{Cu}(\text{dmae})(\text{OCOCH}_3)(\text{H}_2\text{O})]_2$ is linked to another through hydrogen bond and it undergoes facile decomposition at 300 °C to deposit granular copper metal film under nitrogen atmosphere. The decomposition temperature, thermal behaviour, kinetic parameters, evolved gas pattern of the complex, morphology, and the composition of the film were also investigated.

Key Words : Copper, Thin film, Synthesis, TGA/FTIR

Introduction

Chemical Vapour Deposition (CVD) processes have been used in many fields of industrial activity¹⁻³ to deposit films which protect objects from corrosion or abrasion in engineering environments. The industrial fields are diverse and range from gas turbines to nuclear power plants, gas sensors, and catalysts for environmental and industrial utility.⁴⁻⁸ Clearly, the production of a thin layer of metal by CVD strongly depends on experimental parameters such as precursor choice, deposition temperature, flow rate which can have significant impact on the grain size, surface area, intergranular coupling and hence ultimate properties of the protective layer. Indeed, CVD has been noted as a potential solution to many of the current problems associated with the formation of protective coating.

We have thus undertaken a study aimed at evaluating the potential of copper metal thin films as protective layers for industrial utility. To date, the majority of the precursors for the CVD of Cu have been driven by applications in the micro electronics industry,⁹ and have focused on Cu(I) species such as (hfac)Cu(L) (hfac = hexafluoroacetylacetonate, L = PPh₃, H₂C=C(H)SiMe₃ etc), which deposit the metal *via* a disproportionation process ($2\text{Cu}^{\text{I}} \rightarrow \text{Cu}^0 + \text{Cu}^{\text{II}}$). These Cu(I) species are, however, of poor thermal stability and have a tendency to incorporate fluorine into the film from decomposition of the hfac ligand. On the other hand, Cu(II) precursors such as Cu(hfac)₂ are generally more stable but require the addition of a reducing agent (*e.g.* H₂) to get good, contaminant-free films.¹⁰ However, Cu(II) aminoalkoxides, $[\text{Cu}[\text{OCH}(\text{R}^1)\text{CH}_2\text{N}(\text{R}^2)(\text{R}^3)]_2]$,¹¹⁻¹³ have been reported to give copper films without need for an ancillary precursor,¹⁴ in which the aminoalkoxide functions as a reducing agent; an *in situ* IR study has shown that

$\text{Cu}(\text{OCH}_2\text{CH}_2\text{NMe}_2)_2$ generates dimethylaminoethanol and dimethylaminoethanol as by-products.^{15,17}

In the light of these results, we have synthesized an air-stable copper compound, $[\text{Cu}(\text{dmae})(\text{OCOCH}_3)(\text{H}_2\text{O})]_2$ and investigated its potential for copper metal thin films on a soda glass substrate by CVD. This study provides a comparison with the precursors dimethyldiethylaminopropan-1-ol-copper(II) $[(\text{CH}_3)_2\text{Cu}(\text{C}_2\text{H}_5)_2\text{N}(\text{CH}_3)\text{CH}_2\text{CH}_2\text{OH}]$,¹⁶ and bis(*N,N*-dimethylaminoethoxy)-copper(II) $[\text{Cu}(\text{OCH}_2\text{CH}_2\text{N}(\text{CH}_3)_2)_2]$ ¹⁷ which are highly air and moisture sensitive, and have previously been reported as precursors for thin copper films.

Experimental Details

All manipulations were carried out under dry argon using standard Schlenk flask techniques. Copper(II) acetate monohydrate ($\text{Cu}(\text{OCOCH}_3)_2 \cdot \text{H}_2\text{O}$) and *N,N*-dimethylaminoethanol (dmaeH) ($\text{CH}_3)_2\text{NCH}_2\text{CH}_2\text{OH}$) were supplied by Aldrich Chemicals. dmaeH was purified by refluxing over K₂CO₃ for 10 hrs and distilled immediately before use. Elemental analysis was carried out using CHNS-O analyzer EA1112 (Thermo Electron) and Atomic Absorption Analyser (Varian). Thermal decomposition and evolved gas pattern were studied by TGA/SDTA 851^e (Mettler) and Nicolet (Nexus) FTIR spectrometer, respectively. Scanning electron microscopy and EDX were performed on JOEL JSM-5910. XRD patterns of thin film were also studied.

Synthesis of $[\text{Cu}(\text{dmae})(\text{OCOCH}_3)(\text{H}_2\text{O})]_2$. 1.12 mmol (0.24 g) copper(II) acetate monohydrate $[(\text{Cu}(\text{OCOCH}_3)_2 \cdot \text{H}_2\text{O})]$ was taken in a 50 mL Schlenk tube fitted with cold water reflux condenser, inert gas/vacuum line and containing dry toluene (5 mL). *N,N*-dimethylaminoethanol (1.12 mmol, 0.1 mL) was added from a syringe drop by drop under inert

atmosphere of argon gas. The contents were stirred for 2 hrs until Cu(OCOCH₃)₂·H₂O was completely dissolved and further heated to 40°C in an oil bath for another 2 hrs. The resulting solution was filtered *via* a canola and the filtrate was concentrated under vacuum. This was then placed in a refrigerator at -10°C for crystallization. Bluish-green crystals (mp 87°C) were obtained overnight (yield: 80%). Analysis. % found (calculated for C₁₂ H₃₀ Cu₂ N₂ O₈) C, 28.157 (28.53); H, 6.99 (7.01); N, 5.658 (5.87); O, 29.451 (29.12); Cu 27.5 (26.3). IR cm⁻¹: 3700, 3500, 3035, 2953, 2877, 2825, 2783, 2358, 2343, 1793, 1771, 1717, 1537, 1458, 1397, 1375, 1232, 1179, 1135, 1040, 866, 772, 667.

Thin Film Deposition. An Ultrasonic Atomizer (Cole Palmer) fitted with self designed delivery system (Figure 1) was used to generate aerosol and it was sprayed on heated substrate at 300°C. 100 μL solution of [Cu(dmae)(OCOCH₃)(H₂O)]₂, prepared by dissolving 50mg of complex in 100 ml of dry toluene was continuously injected through a control valve and transferred first from piston pump to an ultrasonic atomizer spray nozzle. The nozzle produced an aerosol in an evacuated quartz chamber. The highly pure nitrogen as carrier gas drew the aerosol to a substrate placed at the bottom of a chamber heated at 300°C producing uniform copper nano layer. The waste gases were evacuated and trapped in a liquid nitrogen trap.

Thermal Decomposition Study. TGA study of the complex [Cu(dmae)(OCOCH₃)(H₂O)]₂ was carried out in the temperature range of 25-350°C with an open 70 μL alumina crucible at a heating rate of 15°C/min under continuous flow (40 mL/min.) of dry nitrogen using Mettler Toledo TGA/SDTA 851^c. The purge gas and the evolved gases from the sample were transferred from the TGA through a transfer line thermostated at 250°C in order to avoid any condensation of evolved gases. FTIR scans of evolved matter were taken at *ca.* every twenty second at a resolution rate of 4 cm⁻¹. Scanning Electron Microscopy and EDAX (JOEL JSM-5910) was used to observe the copper surface morphology, and to measure the average particle size and distribution thereof. The identification of deposited crystalline copper film was characterized by Powder X-ray diffractometer (PAN Analytical X' Pert PRO). X-ray single crystallographic data were collected on a Kappa CCD diffractometer at 150(2)K using Mo-k_α radiation (0.71073

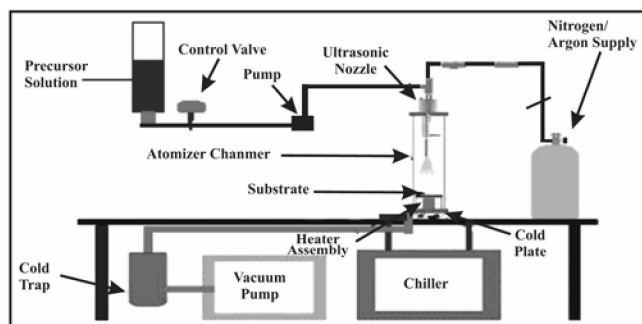


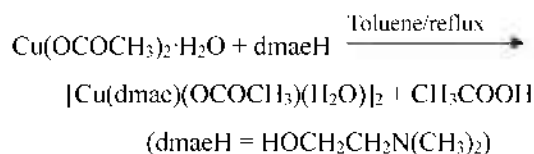
Figure 1. Schematic representation of copper thin film deposition apparatus from [Cu(dmae)(OCOCH₃)(H₂O)]₂.

Å) in the theta range of 4.31 to 30.09° on a crystal of approximate dimensions 0.3 × 0.3 × 0.2 mm. Data were corrected for Lorentz, polarization and absorption; refinement was by full-matrix least-squares on *F*². The largest residual peak/hole was 0.542 and -0.903 eÅ³, respectively.

Crystallographic data for the structures reported here have been deposited with CCDC (Deposition No. CCDC-616085). These data can be obtained free of charge via <http://www.ccdc.cam.ac.uk/conts/retrieving.html> or from CCDC, 12 Union Road, Cambridge CB2 1EZ, UK, email: deposit@ccdc.cam.ac.uk.

Results and Discussion

Copper(II) acetate monohydrate, Cu(OCOCH₃)₂·H₂O reacts in toluene under reflux condition with *N,N*-dimethylaminoethanol(dmaeH) in 1 : 1 molar ratio to give [Cu(dmae)(OCOCH₃)(H₂O)]₂ in 80% yield. Dissolution of Cu(OCOCH₃)₂·H₂O in the reaction mixture indicates completion of the reaction, which proceeded according to the following equation.



The molecular structure of [Cu(dmae)(OCOCH₃)(H₂O)]₂ is shown in Figure 2. Although the lattice can be visualized as being constructed from linking dimers of formula [Cu(dmae)(OCOCH₃)(H₂O)]₂, this belies the complexity of this moiety, as the two metal centers are quite distinct. Cu(1) has a four-coordinated CuO₃N coordination sphere comprising one O,N-chelating dmae, one O-bridging dmae and a monodentate acetate group. The geometry is a distorted square plane [*<*O(1)Cu(1)N(2) 100.61(5), O(1)Cu(1)O(3) 95.22(5), O(3)Cu(1)O(6) 79.16(5)^o, O(6)Cu(1)N(2) 85.05(5)^o]

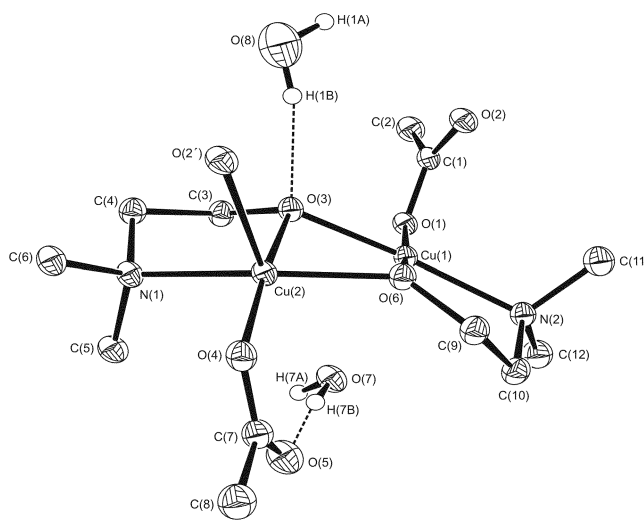


Figure 2. The asymmetric unit of [Cu(dmae)(OCOCH₃)(H₂O)]₂ showing the labeling scheme used in the text and tables: atomic displacements are at the 30% level.

Table 1. Crystal data for $[\text{Cu}(\text{dmae})(\text{OCOCH}_3)(\text{H}_2\text{O})]_2$

Empirical formula	$\text{C}_{12}\text{H}_{30}\text{Cu}_2\text{N}_2\text{O}_8$
Formula weight	457.46
Crystal system	monoclinic
Space group	$P 2_1/c$
a (Å)	8.9270(1)
b (Å)	11.5210(1)
c (Å)	18.1920(2)
β (°)	94.612(1)
V (Å ³)	1864.95(3)
Z	4
Independent reflections	5435 [R(int) = 0.0610]
Reflections observed ($I > 2\sigma$)	4718
Final R1, wR2 [$I > 2\sigma(I)$]	0.0291, 0.0731
Final R1, wR2 (all data)	0.0360, 0.0775

in which O(1)/O(6) and O(3)/N(2) are pairs in mutually trans positions [$\angle\text{O}(1)\text{Cu}(1)\text{O}(6)$ 171.03(5), $\text{O}(3)\text{Cu}(1)\text{N}(2)$ 164.15(5)°]. In contrast, Cu(2) adopts a CuO_3N environment in which a nominally CuO_3N square plane (analogous in origin to that of Cu(1)) is capped by the oxygen of a bridging acetate group O(2') to generate a square pyramidal geometry. Bond angles within the CuO_3N plane are similar to Cu(1) [$\text{O}(3)\text{Cu}(1)\text{N}(1)$ 85.34(5), $\text{N}(1)\text{Cu}(2)\text{O}(4)$ 95.48(5), $\text{O}(4)\text{Cu}(2)\text{O}(6)$ 98.67(5) and $\text{O}(3)\text{Cu}(2)\text{O}(6)$ 78.58(5); $\text{O}(3)\text{Cu}(2)\text{O}(4)$ 172.46(5), $\text{O}(6)\text{Cu}(2)\text{N}(1)$ 158.68(5)°] with the capping O(2') essentially at right angles [angles involving O(2') and Cu(2) 89.99(5)-105.75(5)°]. Two dmae groups link Cu(1) and Cu(2) through bridging oxygen to give a dimer.

While the two dmae ligands behave similarly, the carboxylate groups do not. The acetate centered on Cu(1) is bidentate and bridges the two metal centre; the C-O and C=O bond lengths are distinct [C(1)-O(1) 1.2922(19), C(1)-O(2) 1.2391(19) Å] and it is the shorter CO group which is

involved in the longer, weaker bridging interaction [O(1)-Cu(1) 1.9440(11), O(2')-Cu(2) 2.3781(12) Å]. The second group based on C(7) is monodentate with respect to copper [O(4)-Cu(2) 1.9296(12) Å] but engages in hydrogen bonding with the one of the lattice waters [O(5)⋯H(7A) 1.971 Å, O(5)⋯O(7) 2.844 Å; $\angle\text{O}(5)\text{H}(7\text{A})\text{O}(7)$ 175.7°]. Again, the two C-O bonds are distinct [C(7)-O(4) 1.283(2), C(7)-O(5) 1.237(2) Å], though both carboxylates involve some double bond delocalization as the C-O bonds of the dmae groups are significantly longer [C(3)-O(3) 1.418(2), C(9)-O(6) 1.412(2) Å].

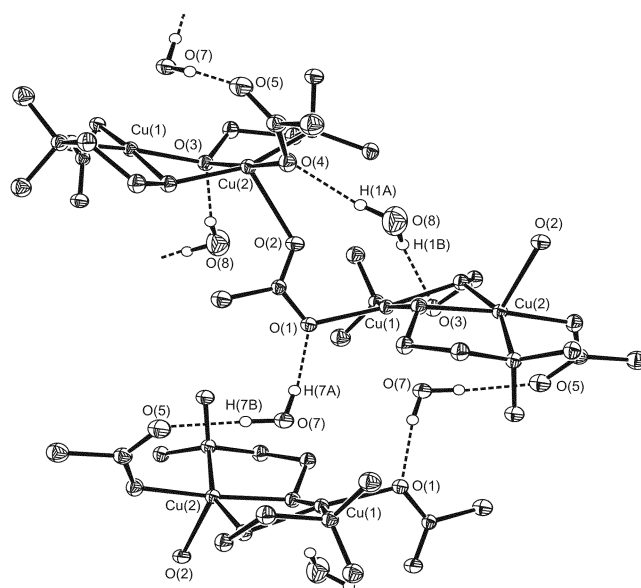
Two water molecules involve themselves in two hydrogen bonds. O(7), in addition to the hydrogen bond to O(5) already mentioned, forms a second hydrogen bond to the acetate group linked to Cu(1) [O(1)⋯H(7B) 1.978 Å, O(1)⋯O(7) 2.845 Å, $\angle\text{O}(1)\text{H}(7\text{B})\text{O}(7)$ 172.0°]. In contrast, O(8) utilizes one acetate [O(4)⋯H(1A) 1.966 Å, O(4)⋯O(8) 2.847 Å, $\angle\text{O}(4)\text{H}(1\text{A})\text{O}(8)$ 171.0°] and one dmae [O(3)⋯H(1B) 1.970 Å, O(3)⋯O(8) 2.836 Å, $\angle\text{O}(3)\text{H}(1\text{B})\text{O}(8)$ 166.2°] as hydrogen bond receptors. The overall lattice structure generated by the combination of bridging acetate and the network of hydrogen bonds is shown in Figure 3.

The combination of TGA/DTG and FTIR provides detailed information on decomposition process. Thermogravimetric analysis (TGA) and derivative thermogravimetric (DTG) curves for decomposition of $[\text{Cu}(\text{dmae})(\text{OCOCH}_3)(\text{H}_2\text{O})]_2$ are shown in Figure 4. A three-step pathway for decomposition is observed with gradual loss of water (found 7.94% calc. 7.9%) at a temperature range of 30-134°C. In the second and third steps a total weight loss of 61.447% is recorded due to elimination of acetate, dimethylethanol amine and *N,N*-dimethylethanal groups. This observation is in line with the FTIR of evolved gas product taken at various time interval as shown in Figure 5. The correlation between

Table 2. Selected geometric data for $[\text{Cu}(\text{dmae})(\text{OCOCH}_3)(\text{H}_2\text{O})]_2$

Bond distances (Å)		Bond angles (°)	
Cu(1)-O(1)	1.9440(11)	O(1)-Cu(1)-O(3)	95.22(5)
Cu(1)-O(3)	1.9597(11)	O(1)-Cu(1)-O(6)	171.03(5)
Cu(1)-O(6)	1.9187(11)	O(1)-Cu(1)-N(2)	100.61(5)
Cu(1)-N(2)	2.0348(14)	O(3)-Cu(1)-O(6)	79.16(5)
Cu(2)-O(2')	2.3781(12)	O(3)-Cu(1)-N(2)	164.15(5)
Cu(2)-O(3)	1.9447(11)	O(6)-Cu(1)-N(2)	85.05(5)
Cu(2)-O(4)	1.9296(12)	O(2')-Cu(2)-O(3)	97.31(5)
Cu(2)-O(6)	1.9577(11)	O(2')-Cu(2)-O(4)	90.19(5)
Cu(2)-N(1)	2.0688(14)	O(2')-Cu(2)-O(6)	105.76(5)
O(1)-C(1)	1.2922(19)	O(2')-Cu(2)-N(1)	89.99(5)
O(2)-C(1)	1.2391(19)	O(3)-Cu(2)-O(4)	172.46(5)
O(4)-C(7)	1.283(2)	O(3)-Cu(2)-O(6)	78.58(5)
O(5)-C(7)	1.237(2)	O(3)-Cu(2)-N(1)	85.34(5)
		O(4)-Cu(2)-O(6)	98.67(5)
		O(4)-Cu(2)-N(1)	95.48(5)
		O(6)-Cu(2)-N(1)	158.68(5)

Symmetry transformation used to generate equivalent atoms: $-x, y-1/2, -z+1/2$

**Figure 3.** The lattice structure of $[\text{Cu}(\text{dmae})(\text{OCOCH}_3)(\text{H}_2\text{O})]_2$ showing dimeric units linking through bridging acetate groups and a network of H-bonds to form polymeric network.

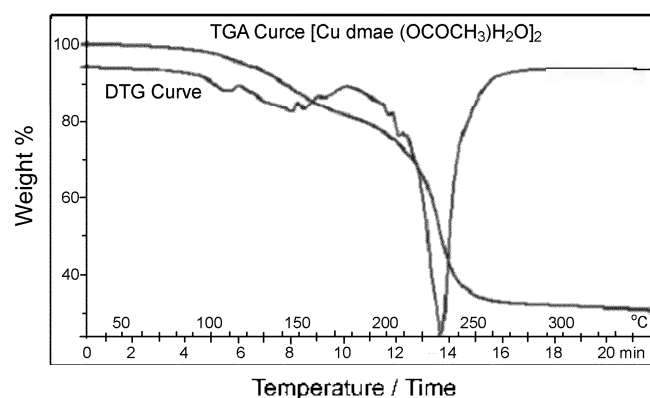


Figure 4. TGA/DTG curve of [Cu(dmae)(OCOCH₃)(H₂O)]₂ at a heating rate of 15°C/min under nitrogen atmosphere at a flow rate of 40 ml./min.

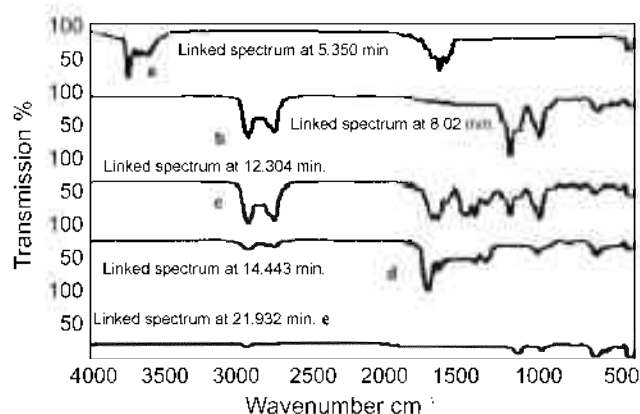
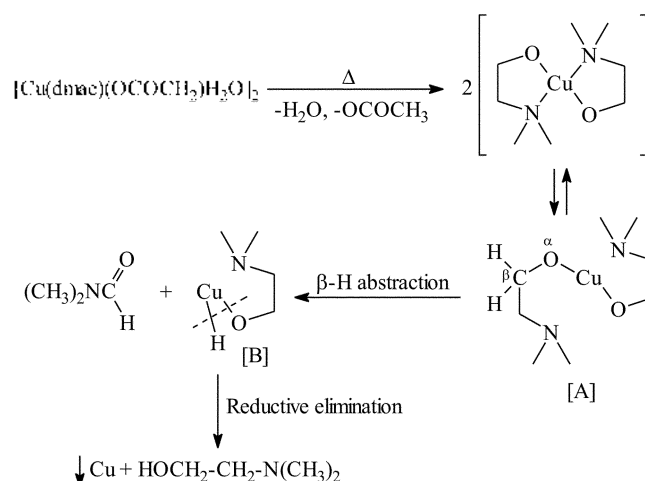


Figure 5. TGA/SDTA Linked FTIR spectra showing systematic decomposition of [Cu(dmae)(OCOCH₃)(H₂O)]₂.

DTG curve and linked FTIR spectrum shows that in the initial 5 minutes (up to 134°C), H₂O is lost, showing absorption at 3700, and 3500 cm⁻¹. The H-O-H bending also gives rise to the absorption at 1717 cm⁻¹. Above 134°C, linked spectra b and c show the elimination of acetate and dmae. This is indicated by the most important vibrational modes of CH₃ stretching around 3035-2953 cm⁻¹, absorption band at 2877 cm⁻¹, the CH₃ asymmetric deformation vibration at 1537-1458 cm⁻¹ followed by symmetric CH₃ vibration at 1397-1375 cm⁻¹. These bands are overlapped with the evolution of dmae and *N,N*-dimethylethanal. In addition to CH₃ stretching, deformation absorption peak, linked spectrum c also shown C=O stretching at 1793-1770 cm⁻¹ of acetate. Absorption near 1750 cm⁻¹ is characteristics of vapour phase aldehyde carbonyl stretch showed the presence of dimethylethanal. The peak at 1232 cm⁻¹ can be reasonably assigned to a C-N stretch of a tertiary *N,N*-dimethylamine.¹⁸ C-O symmetric stretching at 1074-1040 cm⁻¹ is due to presence of R-CH₂-OH group of dmae and thus shows a major loss in weight at DTG maxima. Linked spectrum d confirms the loss of residual product as indicated by the absence of CH₃ stretching absorption band, asymmetric deformation vibration and symmetric vibration, leaving residue of 30.616% against 26.3% of pure copper



Scheme 1. Schematic representation for decomposition of [Cu(dmae)(OCOCH₃)(H₂O)]₂ to copper metal.

plus little impurity of copper oxide. Based on these observations, a pyrolysis mechanism supported by previous work¹⁷ for the decomposition of [Cu(dmae)(OCOCH₃)(H₂O)]₂ to copper metal has been elaborated in Scheme 1. It is reasonable to believe that after the loss of water and acetate molecule in the initial decomposition steps N···Cu bond is opened at higher temperature to liberate species [A] which undergo β -H abstraction to produce species [B] and *N,N*-dimethylaminoethanal. Species [B] readily undergoes reductive elimination to liberate dmaeH and crystalline copper nano particles.

The thermal stability and volatility of [Cu(dmae)(OCOCH₃)(H₂O)]₂ may vary. In toluene solution, the complex has sufficient stability and volatility to serve as a precursor for the deposition of copper nanoparticles, well adherent and without carbon contamination. The decomposition behavior of copper (II) dimethylaminoethoxide, [Cu(dmae)₂]¹⁷ which is sublimable and water-sensitive complex is temperature dependent. Solid thin film grown from this complex at 200 °C consists of copper metal free from any contamination but at 300 °C, the complex yields thin film containing a mixture

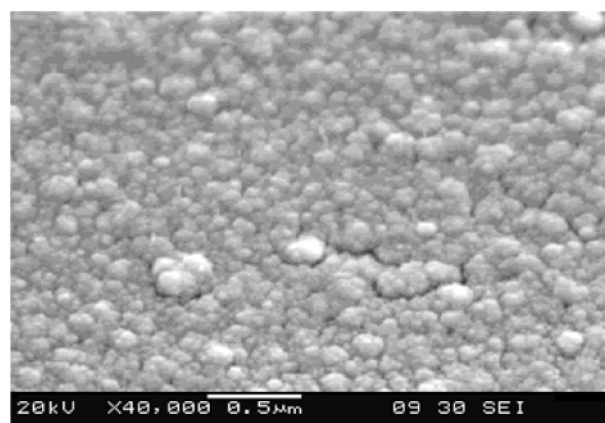


Figure 6. SEM micrograph showing copper metal nano particles ranging from 40-80 nm deposited on soda glass substrate.

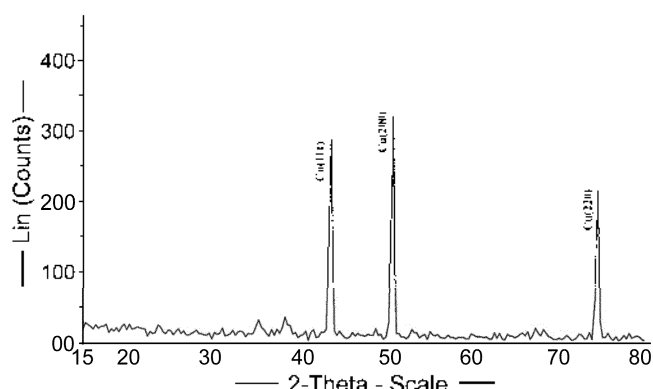


Figure 7. X-ray diffraction pattern of Cu film deposited on soda glass substrate.

of Cu(0), Cu (I) and Cu (II) oxides produced even under nitrogen environment. Figure 6 shows a scanning electron microscopy image of the deposited copper particles. The measurement from the image indicates that these are nano particulate with sizes ranging from 40 nm to 80 nm. These particles make up a film which appears to be uniform and smooth. EDAX analysis confirms that the film comprises of pure copper nanoparticles. XRD pattern of thin film deposited at 300°C under nitrogen environment with a collecting angle varying from 15 to 80° and the usual copper $K\alpha$ radiation $\lambda = 1.5406 \text{ \AA}$ is shown in Figure 7. The hkl values (111), (200), (220), 2θ values 43.4°, 50.6°, 74.3° and corresponding d values, 2.088, 1.805, and 1.278 Å are used for determining lattice parameter which came to be 3.616, 3.616, and 3.616 Å, respectively using standard formula (Lattice = $d\sqrt{h^2+k^2+l^2}$). The relative peak intensities and the position of diffraction peaks in the XRD pattern are very similar to those reported in the JCPDS standard data 4-0836 and others.¹⁹ The position and the integral width of x-ray diffraction peaks are determined to identify the crystalline phase which is found to be face centered cubic. The particle size as calculated by Scherrer equation $Z = K\alpha \lambda / \beta \cos\theta$; where Z is a particle size, β is the value of $\frac{1}{2}$ FWHM (0.1655° rad), θ (25.25°) is half of diffraction angle 2θ , $K\alpha$ (0.9) is a diffraction constant, λ (1.5406) is wavelength of incident light was 55.4 nm and is comparable to 40-80 nm as measured by SEM.

Conclusion

The dimeric complex, $[\text{Cu}(\text{dmae})(\text{OCOCH}_3)(\text{H}_2\text{O})_2]$ was prepared by simple synthetic procedure and characterized by

physio-chemical methods such as m.p determination, elemental analysis and single crystal x-ray analysis.

Decomposition pattern studies of the complex by TGA-FTIR indicated its decomposition behavior to yield metallic copper as a major residue. Thin film having average size 40-80 nm of copper nanoparticle have been successfully deposited on soda glass substrate by AACVD technique which has been characterized by SEM/EDX and confirmed by XRD.

Acknowledgements. The authors MM & SMH are thankful to the Higher Education Commission, Pakistan for its financial support through Project No. 20-91/Acad(R) 103-419.

References

- Hampden-Smith, M. J.; Kodas, T. T. *Chem. Vap. Deposition* **1995**, *1*, 8.
- Hampden-Smith, M. J.; Kodas, T. T. *Chem. Vap. Deposition* **1995**, *1*, 39.
- Maury, F. *J. Phys. II France* **1995**, *5*, C5-449.
- Dossi, C.; Pasaro, R.; Bartsch, A.; Brivio, E.; Galasco, A.; Losi, P. *Catal. Today* **1993**, *17*, 527.
- Dossi, C.; Pasaro, R.; Bartsch, A.; Fusi, A.; Sordelli, L.; Ugo, R.; Ballatreccia, M.; Zanon, R.; Vlaic, G. *J. Catal.* **1994**, *145*, 370.
- Dossi, C.; Pasaro, R.; Sordelli, L.; Ballatreccia, M.; Sordelli, L.; Ballatreccia, M.; Zanon, R. *J. Catal.* **1996**, *159*, 435.
- Dossi, C.; Pasaro, R.; Fusi, A.; Recchia, S.; Sanot, V. dal.; Sordelli, L. *Thermochim. Acta* **1998**, *317*, 157.
- Electroceramic Thin Films*, Part I & II; Auciells, O.; Ramesh, R., Eds.; *MRS Bull.* **1996**, *21*(7).
- Kodas, T. T.; Hampden-Smith, M. J. *The Chemistry of Metal CVD*; VCH: Weinheim, 1994.
- Rickerby, J.; Steinke, J. H. G. *Chem. Revs.* **2002**, *102*, 1525.
- Young, V. L.; Cox, D. F.; Davis, M. E. *Chem. Mater.* **1993**, *5*, 1701.
- Hsu, P. F.; Chi, Y.; Lin, J. W.; Liu, C. S.; Carty, A. J.; Peng, S. M. *Chem. Vap. Deposition* **2001**, *7*, 28.
- Becker, R.; Devi, A.; Weiss, J.; Weckenmann, U.; Winter, M.; Kiener, C.; Becker, H. W.; Fischer, R. A. *Chem. Vap. Deposition* **2003**, *9*, 149.
- Goel, S. C.; Kramer, K. S.; Chiang, M. Y.; Buhro, W. E. *Polyhedron* **1990**, *9*, 611.
- Young, V. L.; Cox, D. F.; Davis, M. E. *Chem. Mater.* **1993**, *5*, 1701.
- Bradlet, D. C.; Mehrotra, R. C.; Gaur, D. P. *Metal Alkoxides*; Academic Press Inc. (London) Ltd.: 1978; p 87.
- Young, V. L.; Cox, D. F.; Davis, M. E. *Chem. Mater.* **1993**, *5*(12), 1701.
- (a) Szymanski, H. A. *A Systematic Approach to the Interpretation of Infrared Spectra*; Hertzillon; Buffalo, NY, 1967. (b) Socrates, G. *Infrared Characteristic Group Frequencies*; John Wiley and Sons: Chichester, 1980.
- Mukhopadhyay, S.; Shalini, K.; Devi, A.; Shivashankar, S. A. *Bull. Mater. Sci.* **2002**, *25*(5), 391.